

# MASKCAPTIONER: LEARNING TO JOINTLY SEGMENT AND CAPTION OBJECT TRAJECTORIES IN VIDEOS

Gabriel Fiastre<sup>1\*</sup>

Antoine Yang<sup>2</sup>

Cordelia Schmid<sup>1</sup>

<sup>1</sup>Inria, École Normale Supérieure, CNRS, PSL Research University <sup>2</sup>Google Deepmind

## ABSTRACT

Dense Video Object Captioning (DVOC) is the task of jointly detecting, tracking, and captioning object trajectories in a video, requiring the ability to understand spatio-temporal details and describe them in natural language. Due to the complexity of the task and the high cost associated with manual annotation, previous approaches resort to disjoint training strategies, potentially leading to suboptimal performance. To circumvent this issue, we propose to generate captions about spatio-temporally localized entities leveraging a state-of-the-art VLM. By extending the LVIS and LV-VIS datasets with our synthetic captions (LVISCap and LV-VISCap), we train MaskCaptioner, an end-to-end model capable of jointly detecting, segmenting, tracking and captioning object trajectories. Moreover, with pretraining on LVISCap and LV-VISCap, MaskCaptioner achieves state-of-the-art DVOC results on three existing benchmarks, VidSTG, VLN and BenSMOT. The datasets and code are available at <https://www.gabriel.fiastre.fr/maskcaptioner/>.

## 1 INTRODUCTION

A fundamental aim of computer vision is to enable machines to understand videos with human-like acuity in perceiving and reasoning about the world. Recent advances have led to remarkable progress in both spatio-temporal localization (Ren et al., 2015; Redmon et al., 2016; Carion et al., 2020; He et al., 2017; Wojke et al., 2017; Zhang et al., 2022b) and vision-language understanding (Vinyals et al., 2015; Sun et al., 2019; Yu et al., 2019; Yang et al., 2021; Chen et al., 2020; Jia et al., 2021; Zellers et al., 2021; Bain et al., 2021; Lu et al., 2019; Kamath et al., 2021). However, building vision-language models that can simultaneously reason about spatially localized objects and temporal dynamics of a complex scene remains a significant challenge, motivated by many real-world applications including autonomous driving (Kim et al., 2019; Atakishiyev et al., 2024), human-computer interaction (Shridhar et al., 2020; Ahn et al., 2022), or video editing (Molad et al., 2023; Jeong and Ye, 2024). Dense Video Object Captioning (DVOC) (Zhou et al., 2025) serves as a key benchmark for this purpose, as it requires to jointly localize, track, and describe in natural language *all* visual entities in a video.

Manual annotation for such a fine-grained task is particularly expensive, leading to a scarcity of datasets with densely annotated object-level video descriptions. To tackle DVOC, prior work resorted to alternative training approaches: Zhou et al. (2025) propose a disjoint training strategy, decomposing the problem into subtasks and training a model sequentially on datasets for each subtask. Choudhuri et al. (2024) leverage the pretraining of multiple specialized models to alleviate the need for object-level annotations. Both methods allowed to perform DVOC while circumventing the need for costly annotations, but the lack of end-to-end training with densely annotated object-level supervision may lead to suboptimal performance.

We propose to address this limitation by generating synthetic object-level annotations, motivated by the recent success of LLM-generated supervision (Liu et al., 2023; Abdin et al., 2024) and the growing visual capacities of Vision Language Models (VLMs) (Alayrac et al., 2022; Li et al., 2022; 2023a; Team et al., 2023; 2024; Achiam et al., 2023; Grattafiori et al., 2024; Bai et al., 2023). To the best of our knowledge, our work is the first to generate localized, object-level captions for DVOC. To this end, we introduce a multi-modal prompting strategy leveraging a state-of-the-art VLM, and

\*Corresponding author: gabriel.fiastre@inria.fr



A person is holding a pencil sharpener in their hands.  
 The black Derwent pencil sharpener is being held and rotated in a person's hand.  
 A graphic pencil with a red end sits on a wooden surface next to a pencil sharpener.

Figure 1: Examples of synthetic captions in our LV-VISCap dataset.

extend two segmentation datasets, LVIS (Gupta et al., 2019) for images and LV-VIS (Wang et al., 2023) for videos, to be the first DVOC training sets with (mask, box, category, caption) annotations for all objects, dubbed LVISCap and LV-VISCap, see figure 1.

Using our generated datasets, we extend the DVOC task, traditionally formulated as detection (Zhou et al., 2025), to segmentation and train MaskCaptioner, the first end-to-end model that can jointly produce (mask, caption) pairs for all object trajectories in a video. We show that (i) our generated datasets, LVISCap and LV-VISCap, largely benefit MaskCaptioner’s DVOC performance, (ii) our MaskCaptioner outperforms previous state-of-the-art models on the VidSTG, VLN and BenSMOT DVOC benchmarks and (iii) we can extend the DVOC task to segmentation.

Overall, our contributions can be summarized as follows:

1. We introduce a VLM-based method to generate synthetic object captions for videos, and extend the LVIS and LV-VIS datasets to be the first unified DVOC training set with object captions, boxes, and segmentation masks: LVISCap and LV-VISCap.
2. Using our unified generated data, we train MaskCaptioner, the first end-to-end model to jointly detect, segment, track and caption objects in a video.
3. MaskCaptioner achieves state-of-the-art DVOC results on the three existing benchmarks : VidSTG, VLN and BenSMOT.

## 2 RELATED WORK

**Open-Vocabulary Video Instance Segmentation (OV-VIS).** The OV-VIS task aims to segment, track, and classify objects from an open set of categories in videos (Guo et al., 2025; Wang et al., 2023), using datasets such as LV-VIS (Wang et al., 2023). State-of-the-art methods (Guo et al., 2025; Wang et al., 2023; Fang et al., 2025) commonly use query-based approaches that classify objects by matching visual features with CLIP embeddings (Radford et al., 2021). Methods like OVFormer (Fang et al., 2025) or BriVIS (Cheng et al., 2025) improve this approach by better aligning visual queries with the CLIP space. Unlike these methods focused on CLIP feature matching for classification, our work explores describing objects in natural language (Li et al., 2023a).

**Localized vision-language understanding.** Going beyond pioneering vision-language tasks such as visual question answering (Antol et al., 2015) or image captioning (Chen et al., 2015), recent work has explored spatial understanding tasks that require localizing natural language queries in images. This includes referred expression segmentation (Kazemzadeh et al., 2014; Yu et al., 2018; Yang et al., 2022b), image grounding (Rohrbach et al., 2016; Plummer et al., 2015), reasoning segmentation (Lai et al., 2024; Wang and Ke, 2024), spatio-temporal video grounding (Zhang et al., 2020; Yang et al., 2022a) and grounded visual question answering (Zhu et al., 2016; Xiao et al., 2024; Lei et al., 2018; 2020). While these tasks typically require localizing one or a few entities, dense captioning (Johnson et al., 2016; Wu et al., 2024) aims to spatially localize and describe in natural language *all* salient regions in images. Our work addresses the more challenging task of predicting *both* object trajectories and descriptions for *all* objects in a video.

**Dense Video Object Captioning (DVOC).** The DVOC task aims at jointly detecting, tracking, and describing the trajectory of all visual entities in a video. DVOC-DS (Zhou et al., 2025) tackles this task by generating frame-wise object box proposals (Zhou et al., 2019; Cai and Vasconcelos, 2018) that are tracked (Zhou et al., 2022) before feeding aggregated and cropped features to a generative image-to-text decoder (Wang et al., 2022). To cope with the lack of DVOC annotations, the model is trained disjointly on various subtasks: object detection using COCO (Lin et al., 2014), image

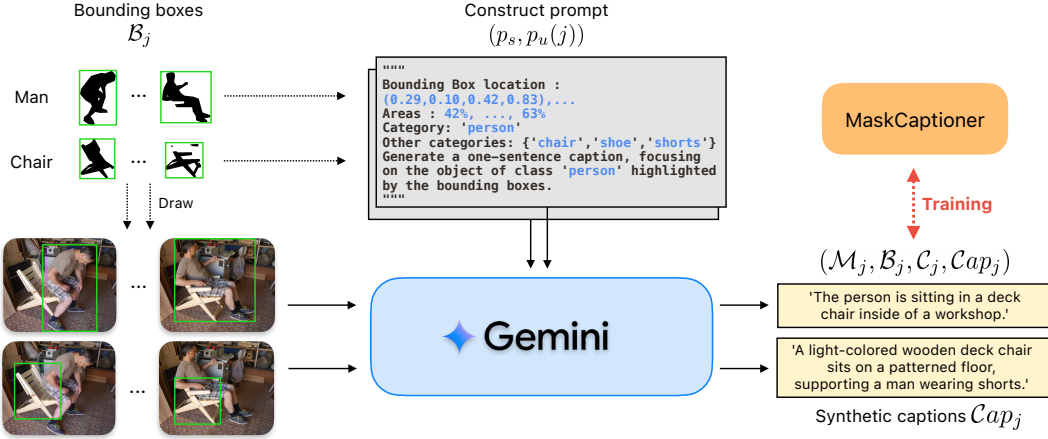


Figure 2: **Our MaskCaptioner data annotation pipeline:** For each object, we extract its bounding boxes  $\mathcal{B}_j$  from its annotated masks  $\mathcal{M}_j$ , and draw them in the video. The video with drawn bounding boxes  $\hat{x}_j$ , along with a prompt  $(p_s, p_u(j))$  including additional information such as the label of the object to caption  $\mathcal{C}_j$ , the labels and bounding boxes of other objects in the image, is fed to a state-of-the-art VLM (Gemini 2.0 Flash (Team et al., 2023)) to generate the object-level caption.  $p_s$  denotes the static prompt with general instructions and  $p_u(j)$  the dynamic prompt with annotation information. We use this pipeline to generate the LVISCap and LV-VISCap datasets, used to train MaskCaptioner.

object-level captioning using Visual Genome (Krishna et al., 2017), video scene-level captioning using SMiT (Monfort et al., 2021) and video object tracking using AugCOCO (Lin et al., 2014). OW-VisCapTor (Choudhuri et al., 2024) extends the DVOC task to segmentation masks. Its architecture relies on an object abstractor using a prompt encoder and transformer blocks, an inter-query contrastive loss to ensure object queries are diverse, and an object-to-text abstractor that connects these queries to a frozen LLM, generating rich, object-centric captions for each detected instance. While proposing to extend DVOC to segmentation, OW-VisCapTor is hindered by the absence of paired (mask, caption) annotations, hence segmentation and DVOC are tackled in isolation using separate models. Closely related, SMOTer (Li et al., 2024) extends multi-object tracking to object-level captioning, video-level captioning and object-relation predictions, and introduce a hand-annotated dataset, BenSMOT. However, BenSMOT focuses on humans only, whereas the standard DVOC task considers all visual entities in the video. In this work, we automatically generate DVOC datasets, LVISCap and LV-VISCap, and train MaskCaptioner, a model that can end-to-end detect, segment, track and caption object trajectories in videos.

**Vision-language data generation.** A promising approach for intricate vision-language tasks is to generate visual annotations using Large Language Models (LLMs) or Vision Language Models (VLMs). LLaVA (Liu et al., 2023) leverages a LLM to generate conversations and detailed descriptions from paired image-text annotations (Chen et al., 2015). This approach has been followed to generate large-scale instruction tuning data for video understanding (Maaz et al., 2024; Li et al., 2023b). Recent research has focused on the generation of spatially grounded text-image data using LLMs/VLMs: Shikra (Chen et al., 2023) generates grounded QA pairs from Flickr30K Entities (Plummer et al., 2015), LLaVA-Grounding (Zhang et al., 2024) and GLaMM (Rasheed et al., 2024) generate grounded conversational data from datasets such as COCO (Lin et al., 2014). Recently, GROVE (Kazakos et al., 2025) extended GLaMM to generate grounded, temporally consistent video captions, extending dense captioning to the video domain. These methods predominantly operate at the scene level and do not produce localized, object-level video descriptions. In contrast, we introduce a multi-modal prompting strategy to leverage VLMs into generating fine-grained captions for individual object trajectories across time. Recently, Yuan et al. (2025) proposed a related VLM-based approach to generate object-level video captions designed for long sentences referring segmentation. Differently, we focus on the task of Dense Video Object Captioning where no text prompt is given to the model.

### 3 METHOD

Dense Video Object Captioning (DVOC) (Zhou et al., 2025) is the task of jointly detecting, tracking and captioning objects trajectories in a video, i.e. producing a (bounding box or mask, caption) pair

---

for each object in a video at each timestamp they appear. Such densely annotated data is lacking for video, as there is currently no available training dataset including captions for all object trajectories in the videos. The spatio-temporal grounding dataset VidSTG (Zhang et al., 2020) has been repurposed to DVOC but only includes annotations for few objects per video and a limited number of frames per video.

We address the lack of data by introducing a strategy for synthetic DVOC data generation, allowing unified training of a DVOC model on (trajectory, caption) pairs for each object, as presented in Section 3.1. With this strategy, we extend the LV-VIS dataset (Wang et al., 2023), which includes both boxes and masks in their (trajectory, label) annotations for all objects, to a variant, dubbed LV-VISCap, which additionally includes synthetically generated captions for each trajectory. To enable end-to-end training on this rich data using segmentation masks, we build an architecture based on a state-of-the-art Open-Vocabulary Video Instance Segmentation (OV-VIS) model OVFormer (Fang et al., 2025), as described in Section 3.2.1. As OVFormer is designed for classification, we extend it with a captioning head (Choudhuri et al., 2024), as explained in Section 3.2.2. Finally, we present in Section 3.3 the losses used to train our model.

### 3.1 DVOC DATA GENERATION

We start from the LV-VIS dataset (Wang et al., 2023) which contains (segmentation masks, category) manual annotations for all objects and timestamps of the videos. To automatically collect DVOC data, one challenge is to generate accurate object-level captions for each trajectory. For this, we leverage a state-of-the-art VLM (Gemini 2.0 Flash (Team et al., 2023)) and feed it with videos where the object to caption is marked with drawn bounding boxes, as illustrated in Figure 2.

**Visual Prompt.** Formally, let  $x \in \mathbb{R}^{N \times H \times W \times 3}$  be a video clip of length  $N$ , with associated mask and category annotations for  $M$  objects in the video:  $(\mathcal{M}_j, \mathcal{C}at_j)$ ,  $j \in 1, \dots, M$ . We first extract bounding boxes annotations from the ground-truth masks,  $\mathcal{B}_j \in \mathbb{R}^{N \times 4}$ ,  $j \in 1, \dots, M$ . We draw each object boxes on a separate copy of the video, and denote as  $a \wedge b$  the operation of drawing box  $b$  on frame  $a$ . We obtain a visual prompt  $\hat{x}_j^i$  for each object trajectory:  $\hat{x}_j^i = x^i \wedge \mathcal{B}_j$  for  $i \in 1, \dots, N$ ,  $j \in 1, \dots, M$

Note that in practice, we subsample  $N$  to 4 uniformly sampled video frames as we found it produces representative enough visual content for the captioning task.

**Text prompts.** In detail, the prompt we feed the VLM is composed of the previously described visual prompt  $\hat{x}_j$ , a system prompt  $p_s$  and a user prompt  $p_u(j)$ . The system prompt is static for all objects/videos and gives general instructions (e.g. "Generate a caption about a queried object highlighted with bounding boxes."), rules (e.g. "Do not mention the bounding boxes in the caption."), format, and an example. The user prompt  $p_u(j)$  however, is constructed for each annotation and enriched with informations about the specific query to help the model. The user prompt encodes textual bounding box coordinates, area, category name of the queried object, and category names from other objects in the image. Passing information through different channels (visual prompt, text prompt) helps the model focusing on the queried object and being accurate when describing the scene. Also, this complementary information can lead the model to reason about the objects (e.g. area being small for an object of category 'elephant' implies the object is most likely part of the background). The different prompting cues have been ablated in Table 1. In particular, showing that including textual semantic and localization cues in the prompt helps the model to focus on the queried object and generate more accurate object-focused captions. We notice that using the segmentation masks as the visual prompt for the model results in less accurate object captions, which might result from a poorer alignment with the localization cues

Table 1: **Impact of the prompting strategy on caption quality.** Scores are given by an expert human evaluator from 0 to 2 (incorrect, partially correct, or correct) on a subset from the LV-VIS validation set, and brought to 0-100 range. For the mask visual prompt experiments, we use our best prompt with either the object’s bounding boxes or center point coordinates as a localization cue in the text prompt.

| Visual prompt   | Prompting method         | Average rating |
|-----------------|--------------------------|----------------|
| bounding boxes  | single frame             | 26.8           |
|                 | + multiple frames        | 27.1           |
|                 | + detailed instructions  | 29.5           |
|                 | + category labels        | 80.7           |
|                 | + bbox coordinates       | 83.1           |
|                 | + bbox area              | 84.3           |
| mask boundaries | + few shot examples      | <b>85.1</b>    |
|                 | center point coordinates | 75.9           |
| mask boundaries | bbox coordinates         | 77.1           |

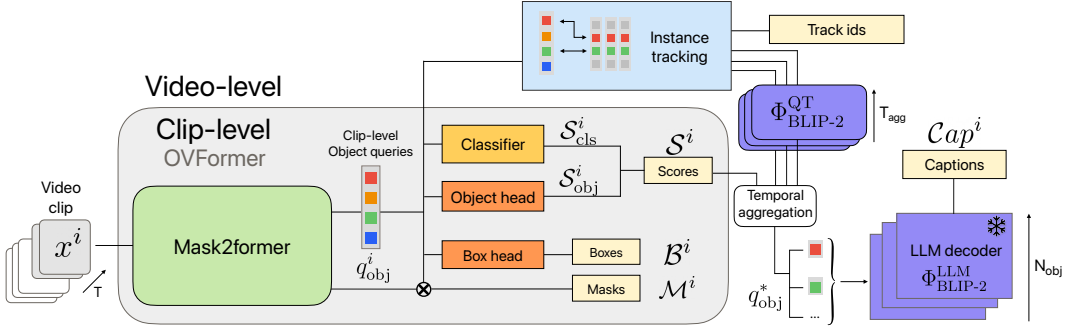


Figure 3: **Our MaskCaptioner architecture** jointly segments and captions objects in videos. For each clip of  $T$  frames, we obtain  $N_{obj}$  clip-level object queries through Mask2Former (Cheng et al., 2021), and yield associated score, mask and box predictions. At a video-level, we match the predicted object queries with the previously processed clips with the Hungarian bipartite matching algorithm, and perform instance tracking (Zhu et al., 2024). For each track, we sample  $T_{agg}$  clips uniformly across the video, and aggregate the tracked queries to obtain a single video query per object, which we can feed to the LLM captioning head (Li et al., 2023a), producing a single caption per trajectory.

included in the text prompt. The full template details for the model prompt construction and a more detailed ablation are given in Appendix A.4.1 and A.2.

**The LVISCap and LV-VISCap datasets.** For each object  $j$  in the video, we prompt Gemini 2.0 Flash (Team et al., 2023) with the visual and textual prompts  $(\hat{x}_j, p_s$  and  $p_u(j))$  to output a synthetic caption  $Cap_j$ . The full DVOC annotation is  $(\mathcal{M}_j, \mathcal{B}_j, Cat_j, Cap_j)$ . We repeat this process for each object in each videos of LV-VIS, generating over 19.5k synthetic captions over 3.9k videos covering 1,020 object classes, and with an average length of 13.9 words. We repeat this process with the LVIS dataset to support image pre-training, applying the same method as above described with each image considered a video of len  $N = 1$ , and obtain our DVOC training sets: LVISCap and LV-VISCap.

### 3.2 MASKCAPTIONER ARCHITECTURE

To enable end-to-end training on the previously described DVOC data including segmentation masks, our architecture, illustrated in Figure 3, processes videos as  $N_{clip}$  clips of  $T$  consecutive frames each, and is composed with: (i) at the clip level, an instance segmentation and detection component, see Section 3.2.1 (ii) at the video-level, a tracking module and a captioning head, see Section 3.2.2.

#### 3.2.1 INSTANCE SEGMENTATION AND DETECTION

**Background: OVFormer (Fang et al., 2025).** Our clip-level instance segmentation component is based on OVFormer (Fang et al., 2025), which we shortly describe next. On a high level, OVFormer augments Mask2Former (Cheng et al., 2021) with a classification head to handle Open-Vocabulary Video Instance Segmentation. Mask2Former learns clip-level object queries with a transformer decoder which cross-attends to the features extracted with a visual backbone and are refined with a pixel decoder. Formally, each clip  $x_{clip}^i \in \mathbb{R}^{T \times 3 \times H \times W}$  is composed of  $T$  consecutive frames for images of resolution  $(H, W)$ , and processed independently by the OVFormer model which outputs clip-level object queries  $q_{obj}^i$ , associated mask predictions  $\mathcal{M}^i$ , classification and objectness scores  $S_{cls}^i$  and  $S_{obj}^i$ :  $(q_{obj}, \mathcal{M}^i, S_{cls}^i, S_{obj}^i) = \Phi_{OVFormer}(x^i)$  where  $q_{obj}^i \in \mathbb{R}^{N_{obj} \times D}$ ,  $\mathcal{M}^i \in \mathbb{R}^{N_{obj} \times T \times H \times W}$ ,  $S_{cls}^i \in \mathbb{R}^{N_{clip} \times N_{obj} \times N_{cls}}$  and  $S_{obj}^i \in \mathbb{R}^{N_{clip} \times N_{obj}}$ .

**Detection head.** We extend this segmentation module with detection by using a 4-layer MLP to generate boxes on top of the object queries  $q_{obj}^i$ :  $\mathcal{B}^i = \text{BoxHead}(q_{obj}^i) \in \mathbb{R}^{N_{obj} \times T \times 4}$ .

**Confidence scores.** Note that OVFormer (Fang et al., 2025) only computes class-aware query-wise confidence scores over the full video. However, for objects appearing only in a small subset of frames in the video this strategy could result in inaccurate scores. Moreover, for DVOC, we wish to avoid redundant predictions i.e. having two queries predicting a similar trajectory. Hence we additionally compute *class-agnostic* query-wise confidence scores for each clip  $S_{cls*}^i$ , by taking the maximum classification score over all labels  $c \in 1, \dots, N_{cls}$  for each query and clip:

---

$S_{\text{cls}*}^i = \max_c(S_{\text{cls}}^i(c)) \in \mathbb{R}^{N_{\text{clip}} \times N_{\text{obj}}}$ . Finally we derive the per-clip score  $\mathcal{S}^i = \sqrt{\mathbf{S}_{\text{cls}*}^i \times \mathbf{S}_{\text{obj}}^i}$  which we use for filtering predictions below a threshold  $t_{\text{thresh}}$  at inference-time for every time step.

### 3.2.2 INSTANCE TRACKING AND CAPTIONING

**Tracking module.** To derive the output video-level trajectories from the clip-level predictions, we need to obtain a matching between the queries at time  $i$  and the queries at time  $i + 1$ . For this, we perform tracking between the clips using the top-K enhanced query-matching module from Zhu et al. (2024). For each clip, this module keeps a memory bank containing the queries from the  $T_{\text{match}}$  previous clips. Among these, it identifies the  $K_{\text{match}}$  most matched clips, and computes the optimal assignment using the Hungarian bipartite matching algorithm. Using the  $K_{\text{match}}$  most matched clips helps reducing error propagation compared to the OVFormer (Fang et al., 2025) tracking module, which maps queries from time  $i + 1$  to time  $i$  directly. Notably, we can keep track of objects that disappear and re-appear in a video, whereas they are automatically lost using the OVFormer tracking module.

This method is referred to as semi-online tracking as we represent objects at a clip-level and associate between the clips in an online fashion. This offers the advantages of being flexible (fully-online for clips of length  $T = 1$ ) and to arbitrate between using multi-frame information and memory constraints for long videos.

**Captioning head.** To caption tracked object trajectories, we adapt the captioning head from Choudhuri et al. (2024) based on BLIP-2 (Li et al., 2023a). The BLIP-2 decoder processes object queries one by one using masked-attention conditioned with the predicted masks, before projecting the resulting object query into the LLM space for caption prediction. However, for consistency and efficiency, we predict a single video-level caption per tracked object query, replacing clip-level prediction.

**Query aggregation.** Let's consider  $\Phi_{\text{BLIP2}}^{\text{QT}}$  the BLIP-2 query transformer,  $\Phi_{\text{BLIP2}}^{\text{LLM}}$  the LLM decoder,  $q_{\text{obj}}^i(j) \in \mathbb{R}^{1 \times D}$  and  $\mathcal{S}_{\text{obj}}^i(j) \in \mathbb{R}$  respectively the query and the detection score for object  $j$  from clip  $i$ . For each object, we aggregate the tracked queries over time after they are processed by the BLIP-2 query transformer, by sampling a set  $\mathcal{I}_{\text{agg}}$  of  $T_{\text{agg}}$  clips uniformly across the video. We obtain a video query for each object  $j$ :  $q_{\text{obj}}^*(j) = \sum_{i \in \mathcal{I}_{\text{agg}}} \mathcal{S}^i(j) \times \Phi_{\text{BLIP2}}^{\text{QT}}(q_{\text{obj}}^i(j), \mathcal{M}_j^i)$ . We can compute the video captioning prediction for the tracked object:  $\text{Cap}(j) = \Phi_{\text{BLIP2}}^{\text{LLM}}(q_{\text{obj}}^*(j))$  for  $j \in 1, \dots, N$ .

### 3.3 MODEL TRAINING

We train MaskCaptioner with a combination of clip-level and video-level losses. For each clip, we predict masks/boxes, classification scores and captions, and derive the clip-level training objective as the following combination of supervised losses:

$$\mathcal{L}_{\text{clip-level}} = \mathcal{L}_{\text{seg}} + \mathcal{L}_{\text{det}} + \mathcal{L}_{\text{s}} + \mathcal{L}_{\text{cap}} \quad (1)$$

where  $\mathcal{L}_{\text{seg}}$  and  $\mathcal{L}_{\text{s}}$  are the VIS losses from Fang et al. (2025), i.e.  $\mathcal{L}_{\text{seg}} = \lambda_{\text{dice}} \mathcal{L}_{\text{dice}} + \lambda_{\text{ce}} \mathcal{L}_{\text{ce}}$ , with  $\mathcal{L}_{\text{dice}}$  and  $\mathcal{L}_{\text{ce}}$  the dice and cross-entropy segmentation losses respectively, and  $\mathcal{L}_{\text{s}} = \lambda_{\text{cls}} \mathcal{L}_{\text{cls}} + \lambda_{\text{obj}} \mathcal{L}_{\text{obj}}$  where  $\mathcal{L}_{\text{cls}}$  and  $\mathcal{L}_{\text{obj}}$  are the cross-entropy losses for classification and objectness. We add detection and captioning losses  $\mathcal{L}_{\text{det}} = \lambda_{l_1} \mathcal{L}_{l_1} + \lambda_{\text{giou}} \mathcal{L}_{\text{giou}}$  where  $\mathcal{L}_{l_1}$  and  $\mathcal{L}_{\text{giou}}$  are detection losses from Yang et al. (2022a), and  $\mathcal{L}_{\text{cap}} = \lambda_{\text{clip-lm}} \mathcal{L}_{\text{lm}}$ , with  $\mathcal{L}_{\text{lm}}$  the cross-entropy language modeling loss (Zhou et al., 2025).

When including the temporal aggregation module for captioning, we train the captioning head at the video level, i.e. we predict a caption per object for the full video after the tracking is performed and each object-query has been augmented across time.

$$\mathcal{L}_{\text{video-level}} = \lambda_{\text{vid-lm}} \mathcal{L}_{\text{lm}} \quad (2)$$

MaskCaptioner can be trained in a completely end-to-end manner. However, in practice, we train the model in two-stages for most of the experiments to alleviate memory constraints: we first train the segmentation/detection and classification model, then freeze it and tune the captioning head. The captioning head is trained either at the clip-level, or at the video-level when enabling the temporal aggregation module (i.e.  $\lambda_{\text{clip-lm}} = 0$  or  $\lambda_{\text{vid-lm}} = 0$ ). For each loss when they are computed we set their respective weights to  $\lambda_{\text{dice}}, \lambda_{\text{ce}}, \lambda_{l_1} = 5, \lambda_{\text{giou}}, \lambda_{\text{cls}}, \lambda_{\text{obj}} = 2$ , and  $(\lambda_{\text{clip-lm}} = 1 \text{ or } \lambda_{\text{vid-lm}} = 1)$ .

---

## 4 EXPERIMENTS

### 4.1 EXPERIMENTAL SETTING

**Datasets.** **LVIS** (Gupta et al., 2019) and **LV-VIS** (Wang et al., 2023) are large-vocabulary instance segmentation datasets, respectively for image and video. **LVISCap** and **LV-VISCap** denote our extensions of LVIS and LV-VIS (see Section 3.1), with respectively 1,2M/244k synthetic image object captions for the training/validation of LVISCap and 16k/3.7k synthetic video object captions for LV-VISCap (average of 5.4 objects per video). Note that in the absence of annotations on the test sets of LVIS and LV-VIS, we only extend the training and validation sets with captions, and use the validation set for evaluation.

**Benchmarks.** **VidSTG** (Zhang et al., 2020) is a spatio-temporal video grounding dataset containing text descriptions serving as queries, which Zhou et al. (2025) propose to use for DVOC evaluation. The repurposed training and validation sets count 5.4k/602 videos for 15.1k/1.6k object trajectories with captions respectively. **Video Localized Narratives (VNL)** is similarly repurposed (Zhou et al., 2025). For each of the 5.1k training and 2.4k validation videos, the dataset contains 3 sparsely annotated frames with non exhaustive captions. **BenSMOT** contains bounding box trajectories and associated captions focusing exclusively on humans in videos, with an average of 2.2 instances per video. It counts 2.2k videos for training and 1k for evaluation. More details about the datasets are given in Appendix A.4.2.

**Evaluation Metrics.** Following prior work, we evaluate DVOC using the CHOTA metric introduced by Zhou et al. (2025), which extends the widely used multi-object tracking HOTA metric (Luiten et al., 2021). CHOTA decomposes the DVOC task into three components: detection accuracy (DetA) (Luiten et al., 2021), association accuracy (AssA) (Luiten et al., 2021), and captioning accuracy (CapA) (Zhou et al., 2025). These components reflect the model’s ability to (i) correctly localize objects, (ii) maintain their identity across frames, and (iii) generate accurate natural language descriptions. CHOTA is defined as the geometric mean of the three components:  $\text{CHOTA} = \sqrt[3]{\text{DetA} \cdot \text{AssA} \cdot \text{CapA}}$ .

Matching between predicted and ground-truth trajectories is performed using Intersection-over-Union (IoU) thresholds, similarly to standard tracking evaluations (Milan et al., 2016). To extend the metric to segmentation masks, we simply replace box-based IoU with mask-based IoU when computing CHOTA with segmentation masks.

**Implementation details.** Following OVFormer (Fang et al., 2025) we used ResNet50 (He et al., 2016) and SwinBase (Liu et al., 2021) visual backbones. Our Mask2former (Cheng et al., 2022) transformer decoder has 11 layers, and our captioning head is based on the BLIP-2 (Li et al., 2023a) decoder with OPT-2.7B LLM (Zhang et al., 2022a). For LV-VIS experiments we tune the model end-to-end with clip-level supervision only. For other experiments, we first train the segmentation/detection model, then freeze it and tune the captioning head. For VidSTG, VNL and BenSMOT experiments we use video-level tuning for captioning with temporal aggregation. For the largest dataset (COCO + LVIS) the optimization takes 2 days on 4 H100 GPUs. More implementation details and hyper-parameters for different experiments are given in Appendix A.4.3.

### 4.2 RESULTS

#### 4.2.1 BENEFITS OF TRAINING ON LVISCAP AND LV-VISCAP

We first study the impact of integrating our generated datasets for DVOC training in Table 2. We train MaskCaptioner on our synthetic video set, LV-VISCap, and progressively add LVISCap image pretraining. Results are reported on the LV-VISCap validation set. First, we observe that MaskCaptioner achieves strong DVOC results with training only on LVISCap or LV-VISCap, demonstrating the effectiveness of our architecture. Importantly, combining both LVISCap and LV-VISCap leads to best results, showing the benefit of both our generated datasets. Moreover, we observe that our MaskCaptioner is robust to the choice of the visual backbone. Note that the AssA score depends on the detections, hence a worse DetA score with lower recall but higher precision can make the tracking easier: this explains the higher AssA score from the model without LV-VISCap tuning. In Fig. 4, we show that the CapA performance is logarithmically correlated with the quantity of training captions, suggesting that generating more data with our approach might bring further improvements.

Table 2: **Impact of training with LVISCap and LV-VISCap and of the visual backbone on LV-VISCap DVOC.**

| Backbone | LVISCap | LV-VISCap | CapA        | DetA        | AssA        | CHOTA       |
|----------|---------|-----------|-------------|-------------|-------------|-------------|
| SwinB    | -       | ✓         | 37.9        | 48.1        | 89.5        | 54.7        |
|          | ✓       | -         | 30.0        | 34.3        | <b>93.2</b> | 45.8        |
|          | ✓       | ✓         | <b>43.6</b> | <b>54.3</b> | 89.1        | <b>59.5</b> |
| ResNet50 | ✓       | ✓         | 39.0        | 51.1        | 88.5        | 56.1        |

#### 4.2.2 COMPARISON WITH THE STATE OF THE ART

We compare MaskCaptioner to state-of-the-art DVOC methods following the standard evaluation protocol on three existing benchmarks : VidSTG in Table 3, VLN in Table 4 and BenSMOT in Table 5. DVOC-DS (Zhou et al., 2025) reports results without pretraining, and with their disjoint training training strategy, while OW-VISCap (Choudhuri et al., 2024) leverages Mask2former pretrained on COCO for instance segmentation. In Table 3, we include results with the same pretraining data as these methods and show the impact of using our data instead. Pretraining MaskCaptioner on COCO yields better detection and tracking compared to OW-VISCap but comparable captioning performance due to the similar captioning head design. Including our data leads to an improvement on all metrics and especially captioning with a 6.7 CapA increase (15% relative improvement). When pretraining on the disjoint DVOC-DS set, we observe a substantial gain in the captioning metric due to the model design. Moreover, we show that using our pretraining sets results in a further performance improvement, while additionally allowing a unified, much faster training (2032 GPU hours (Zhou et al., 2025) vs 208 for our approach). Moreover, our proposed approach can output segmentation masks unlike the other methods.

Table 3: **Comparison with the state of the art on VidSTG DVOC validation set.** All models are finetuned on VidSTG. "temp. agg." refers to including query temporal aggregation.

| Method                             | Pretraining set            | CapA        | DetA        | AssA        | CHOTA       |
|------------------------------------|----------------------------|-------------|-------------|-------------|-------------|
| OW-VISCap (Choudhuri et al., 2024) | COCO                       | 43.9        | 60.1        | 54.0        | 53.0        |
| MaskCaptioner (ours)               |                            | 44.3        | 65.1        | 70.2        | 58.7        |
| DVOC-DS (Zhou et al., 2025)        | COCO + VG + SMIT + AugCOCO | 39.7        | 65.8        | 70.4        | 56.9        |
| MaskCaptioner (ours)               |                            | 50.1        | 65.0        | 69.2        | 60.9        |
| MaskCaptioner (ours)<br>+ temp agg | COCO + LVISCap + LV-VISCap | 51.0        | <b>66.8</b> | <b>71.0</b> | 62.3        |
|                                    | COCO + LVISCap + LV-VISCap | <b>55.4</b> | <b>66.8</b> | <b>71.0</b> | <b>64.0</b> |

Table 4: **Comparison with state of the art on the VLN DVOC validation set.** Mask loss refers to using the segmentation masks in the detection loss. All models are finetuned on VLN. "temp. agg." refers to including query temporal aggregation.

| Method                             | Mask loss | CapA        | DetA        | AssA        | CHOTA       |
|------------------------------------|-----------|-------------|-------------|-------------|-------------|
| DVOC-DS (Zhou et al., 2025)        | -         | 17.7        | 44.3        | 89.5        | 41.3        |
| MaskCaptioner (ours)               | -         | 21.4        | 48.7        | 89.7        | 45.4        |
| MaskCaptioner (ours)<br>+ temp agg | ✓         | 22.9        | <b>50.1</b> | <b>92.7</b> | 47.4        |
|                                    | ✓         | <b>23.4</b> | <b>50.1</b> | <b>92.7</b> | <b>47.7</b> |

We further evaluate MaskCaptioner on VLN in Table 4 and BensMOT in Table 5. On both benchmarks, our approach improves the detection while the tracking remains competitive. Most important, the

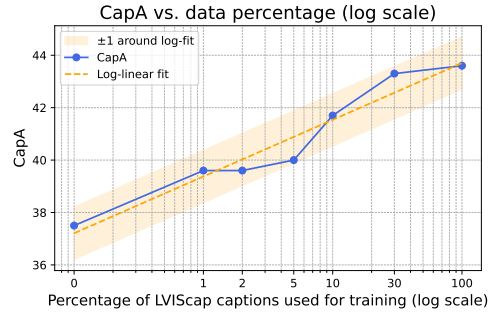


Figure 4: **Impact of the generated data scale on the CapA metric.** We train MaskCaptioner on a varying percentage of LVISCap captions and finetune on LV-VISCap. Captions are used for training.

Table 5: **Comparison on the BenSMOT validation set.** CapA, and thus CHOTA are not reported on this dataset. All models are finetuned on BenSMOT. "temp. agg." refers to including query temporal aggregation.

| Method                             | DetA        | AssA        | CIDEr       |
|------------------------------------|-------------|-------------|-------------|
| SMOTer (Li et al., 2024)           | 80.8        | 73.7        | 8.7         |
| DVOC-DS (Zhou et al., 2025)        | 90.8        | <b>89.6</b> | 25.4        |
| MaskCaptioner (ours)<br>+ temp agg | <b>91.6</b> | 87.5        | 39.9        |
|                                    | <b>91.6</b> | 87.5        | <b>42.6</b> |

Table 6: **Automatic vs manual annotations for evaluation on a subset from LV-VISCap validation** with 50 videos and 233 objects trajectories ; "automatic" and "manual" annotations stands for synthetic or human annotated captions. All models are trained on LVISCap and tuned on our LV-VISCap training set.

| Annotation type | LVISCap captions | CapA        | DetA        | AssA        | CHOTA       |
|-----------------|------------------|-------------|-------------|-------------|-------------|
| automatic       | -                | 33.0        | 48.4        | 89.6        | 52.3        |
|                 | ✓                | <b>40.5</b> | <b>50.0</b> | <b>91.0</b> | <b>56.7</b> |
| manual          | -                | 22.5        | 48.4        | 89.6        | 46.0        |
|                 | ✓                | <b>33.2</b> | <b>50.0</b> | <b>91.0</b> | <b>53.1</b> |

Table 7: **Impact of the inference clip on LV-VISCap.**  
All models are trained on LVISCap then LV-VISCap training set.

| Clip length | mAP         |
|-------------|-------------|
| 3           | 26.0        |
| 4           | 26.1        |
| 5           | <u>26.6</u> |
| 6           | 26.3        |
| 7           | <b>26.8</b> |

captioning metrics improve by a large margin (+5.2 CapA on VLN, +14.7 CIDEr on BenSMOT compared to state of the art). Additionally, our method is able to jointly segment objects, which further improves the performance as shown in Table 4.

Across all benchmarks, we show that including temporal aggregation further improves captioning performance by effectively merging information from multiple video clips, permitting the description of temporally extended actions. We observe only a marginal improvement on VLN, likely due to the short video lengths of this dataset. Because we do not modify the detection and tracking models when adding temporal aggregation, the DetA and AssA scores are unchanged.

#### 4.2.3 ADDITIONAL ABLATIONS

**Annotation bias.** To evaluate the bias introduced by evaluating on LV-VISCap synthetic captions (see Table 2), we annotate a representative subset of our LV-VISCap datasets by hand and compare the impact of our LVISCap captions when evaluating MaskCaptioner on *automatic* vs *manual* data. Our subset comports 50 videos from the LV-VISCap validation set with 233 object trajectories annotated by hand. The results are presented in Table 6. We observe that both the evaluation on automatic and manual data show a comparable improvement on the CapA and CHOTA metric when using our LVISCap captions for the training. This result confirms the importance of our synthetic captions for DVOC performance, and further shows that the bias introduced by evaluating on synthetic LV-VISCap captions is marginal.

**Clip length.** We show in Table 7 the impact of the clip length used for the MaskCaptioner inference. A higher clip length leads to temporally richer queries, improving detection and tracking. Note that in our implementation, we follow OVFormer (Fang et al., 2025) and use a clip length of  $T = 5$ .

**Temporal aggregation.** We show the impact of temporal aggregation on DVOC performance in Table 8. Increasing the number of clips for aggregation consistently improves the captioning scores at the expense of higher training cost. Due to memory constraints we train with a maximum of 32 clips for aggregation on VidSTG. Weighting the clips for aggregation using the detection scores yields a clear improvement over the arithmetic mean. We also observe that performing captioning based on the single clip with best score performs relatively well, which highlights the limits of the complexity of the actions observable in the current benchmarks, e.g. VidSTG (Zhang et al., 2020).

**Additional results.** We show additional results about the prompt ablation and the impact of the tracking module in Appendix A.2. We add MaskCaptioner qualitative examples in Appendix A.1, and discuss the failure cases and limitations of our method in Appendix A.3, as well as give further implementation details in Appendix A.4.

---

## 5 CONCLUSION

We propose an approach to generate synthetic object-level captions using a state-of-the-art VLM and extend the LVIS and LV-VIS datasets with synthetic captions. We use the resulting LVISCap and LV-VISCap datasets to train MaskCaptioner, a DVOC model that can simultaneously detect, segment, track, and caption objects throughout a video. With finetuning, MaskCaptioner achieves state-of-the-art performance on the VidSTG, VLN and BenSMOT benchmarks, while extending the DVOC task to segmentation masks.

## ACKNOWLEDGEMENTS

This work was granted access to the HPC resources of IDRIS under the allocation AD011014323R2 made by GENCI. It was funded in part by the French government under management of Agence Nationale de la Recherche as part of the “France 2030” program, reference ANR-23-IACL-0008 (PR[AI]RIE-PSAI project), the ANR project VideoPredict ANR-21-FAI1-0002-01. Cordelia Schmid would like to acknowledge the support by the Körber European Science Prize.

## REFERENCES

Marah Abdin, Jyoti Aneja, Hany Awadalla, Ahmed Awadallah, Ammar Ahmad Awan, Nguyen Bach, Amit Bahree, Arash Bakhtiari, Jianmin Bao, Harkirat Behl, et al. Phi-3 technical report: A highly capable language model locally on your phone. *arXiv preprint arXiv:2404.14219*, 2024.

Josh Achiam, Steven Adler, Sandhini Agarwal, Lama Ahmad, Ilge Akkaya, Florencia Leoni Aleman, Diogo Almeida, Janko Altenschmidt, Sam Altman, Shyamal Anadkat, et al. GPT-4 technical report. *arXiv preprint arXiv:2303.08774*, 2023.

Michael Ahn, Anthony Brohan, Noah Brown, Yevgen Chebotar, Omar Cortes, Byron David, Chelsea Finn, Chuyuan Fu, Keerthana Gopalakrishnan, Karol Hausman, et al. Do as I can, not as I say: Grounding language in robotic affordances. *arXiv preprint arXiv:2204.01691*, 2022.

Jean-Baptiste Alayrac, Jeff Donahue, Pauline Luc, Antoine Miech, Iain Barr, Yana Hasson, Karel Lenc, Arthur Mensch, Katherine Millican, Malcolm Reynolds, et al. Flamingo: a visual language model for few-shot learning. In *NeurIPS*, 2022.

Stanislaw Antol, Aishwarya Agrawal, Jiasen Lu, Margaret Mitchell, Dhruv Batra, C Lawrence Zitnick, and Devi Parikh. VQA: Visual question answering. In *ICCV*, 2015.

Shahin Atakishiyev, Mohammad Salameh, Hengshuai Yao, and Randy Goebel. Explainable artificial intelligence for autonomous driving: A comprehensive overview and field guide for future research directions. *IEEE Access*, 2024.

Jinze Bai, Shuai Bai, Yunfei Chu, Zeyu Cui, Kai Dang, Xiaodong Deng, Yang Fan, Wenbin Ge, Yu Han, Fei Huang, et al. Qwen technical report. *arXiv preprint arXiv:2309.16609*, 2023.

Max Bain, Arsha Nagrani, Gü̈l Varol, and Andrew Zisserman. Frozen in time: A joint video and image encoder for end-to-end retrieval. In *ICCV*, 2021.

Zhaowei Cai and Nuno Vasconcelos. Cascade R-CNN: Delving into high quality object detection. In *CVPR*, 2018.

Nicolas Carion, Francisco Massa, Gabriel Synnaeve, Nicolas Usunier, Alexander Kirillov, and Sergey Zagoruyko. End-to-end object detection with transformers. In *ECCV*, 2020.

Keqin Chen, Zhao Zhang, Weili Zeng, Richong Zhang, Feng Zhu, and Rui Zhao. Shikra: Unleashing multimodal LLM’s referential dialogue magic. *arXiv preprint arXiv:2306.15195*, 2023.

Xinlei Chen, Hao Fang, Tsung-Yi Lin, Ramakrishna Vedantam, Saurabh Gupta, Piotr Dollár, and C Lawrence Zitnick. Microsoft COCO Captions: Data collection and evaluation server. *arXiv preprint arXiv:1504.00325*, 2015.

---

Yen-Chun Chen, Linjie Li, Licheng Yu, Ahmed El Kholy, Faisal Ahmed, Zhe Gan, Yu Cheng, and Jingjing Liu. UNITER: UNiversal Image-Text Representation learning. In *ECCV*, 2020.

Bowen Cheng, Anwesa Choudhuri, Ishan Misra, Alexander Kirillov, Rohit Girdhar, and Alexander G. Schwing. Mask2Former for video instance segmentation. *arXiv preprint arXiv:2112.10764*, 2021.

Bowen Cheng, Ishan Misra, Alexander G. Schwing, Alexander Kirillov, and Rohit Girdhar. Masked-attention mask transformer for universal image segmentation. In *CVPR*, 2022.

Zesen Cheng, Kehan Li, Li Hao, Peng Jin, Xiawu Zheng, Chang Liu, and Jie Chen. Aligning instance brownian bridge with texts for open-vocabulary video instance segmentation. In *AAAI*, 2025.

Anwesa Choudhuri, Girish Chowdhary, and Alex Schwing. OW-VISCapTor: Abstractors for open-world video instance segmentation and captioning. In *NeurIPS*, 2024.

Jia Deng, Wei Dong, Richard Socher, Li-Jia Li, Kai Li, and Li Fei-Fei. ImageNet: A large-scale hierarchical image database. In *CVPR*, 2009.

Hao Fang, Peng Wu, Yawei Li, Xinxin Zhang, and Xiankai Lu. Unified embedding alignment for open-vocabulary video instance segmentation. In *ECCV*, 2025.

Aaron Grattafiori, Abhimanyu Dubey, Abhinav Jauhri, Abhinav Pandey, Abhishek Kadian, Ahmad Al-Dahle, Aiesha Letman, Akhil Mathur, Alan Schelten, Alex Vaughan, et al. The Llama 3 herd of models. *arXiv preprint arXiv:2407.21783*, 2024.

Pinxue Guo, Hao Huang, Peiyang He, Xuefeng Liu, Tianjun Xiao, and Wenqiang Zhang. OpenVIS: Open-vocabulary video instance segmentation. In *AAAI*, 2025.

Agrim Gupta, Piotr Dollar, and Ross Girshick. LVIS: A dataset for large vocabulary instance segmentation. In *CVPR*, 2019.

Kaiming He, Xiangyu Zhang, Shaoqing Ren, and Jian Sun. Deep residual learning for image recognition. In *CVPR*, 2016.

Kaiming He, Georgia Gkioxari, Piotr Dollár, and Ross Girshick. Mask R-CNN. In *ICCV*, 2017.

Hyeonho Jeong and Jong Chul Ye. Ground-a-video: Zero-shot grounded video editing using text-to-image diffusion models. In *ICLR*, 2024.

Chao Jia, Yinfei Yang, Ye Xia, Yi-Ting Chen, Zarana Parekh, Hieu Pham, Quoc Le, Yun-Hsuan Sung, Zhen Li, and Tom Duerig. Scaling up visual and vision-language representation learning with noisy text supervision. In *ICML*, 2021.

Justin Johnson, Andrej Karpathy, and Li Fei-Fei. Densecap: Fully convolutional localization networks for dense captioning. In *CVPR*, 2016.

Aishwarya Kamath, Mannat Singh, Yann LeCun, Gabriel Synnaeve, Ishan Misra, and Nicolas Carion. MDETR - Modulated detection for end-to-end multi-modal understanding. In *ICCV*, 2021.

Evangelos Kazakos, Cordelia Schmid, and Josef Sivic. Large-scale pre-training for grounded video caption generation. In *ICCV*, 2025.

Sahar Kazemzadeh, Vicente Ordonez, Mark Matten, and Tamara Berg. ReferItGame: Referring to objects in photographs of natural scenes. In *EMNLP*, 2014.

Jinkyu Kim, Teruhisa Misu, Yi-Ting Chen, Ashish Tawari, and John Canny. Grounding human-to-vehicle advice for self-driving vehicles. In *CVPR*, 2019.

Ranjay Krishna, Yuke Zhu, Oliver Groth, Justin Johnson, Kenji Hata, Joshua Kravitz, Stephanie Chen, Yannis Kalantidis, Li-Jia Li, David A Shamma, et al. Visual Genome: Connecting language and vision using crowdsourced dense image annotations. In *IJCV*, 2017.

Xin Lai, Zhuotao Tian, Yukang Chen, Yanwei Li, Yuhui Yuan, Shu Liu, and Jiaya Jia. LISA: Reasoning segmentation via large language model. In *CVPR*, 2024.

---

Jie Lei, Licheng Yu, Mohit Bansal, and Tamara L Berg. TVQA: Localized, compositional video question answering. In *EMNLP*, 2018.

Jie Lei, Licheng Yu, Tamara L Berg, and Mohit Bansal. TVQA+: Spatio-temporal grounding for video question answering. In *ACL*, 2020.

Junnan Li, Dongxu Li, Caiming Xiong, and Steven Hoi. BLIP: Bootstrapping language-image pre-training for unified vision-language understanding and generation. In *ICML*, 2022.

Junnan Li, Dongxu Li, Silvio Savarese, and Steven Hoi. BLIP-2: Bootstrapping language-image pre-training with frozen image encoders and large language models. In *ICML*, 2023a.

KunChang Li, Yinan He, Yi Wang, Yizhuo Li, Wenhui Wang, Ping Luo, Yali Wang, Limin Wang, and Yu Qiao. VideoChat: Chat-centric video understanding. In *CoRR*, 2023b.

Yunhao Li, Qin Li, Hao Wang, Xue Ma, Jiali Yao, Shaohua Dong, Heng Fan, and Libo Zhang. Beyond MOT: Semantic multi-object tracking. In *ECCV*, 2024.

Tsung-Yi Lin, Michael Maire, Serge Belongie, James Hays, Pietro Perona, Deva Ramanan, Piotr Dollár, and C Lawrence Zitnick. Microsoft COCO: Common objects in context. In *ECCV*, 2014.

Haotian Liu, Chunyuan Li, Qingyang Wu, and Yong Jae Lee. Visual instruction tuning. In *NeurIPS*, 2023.

Ze Liu, Yutong Lin, Yue Cao, Han Hu, Yixuan Wei, Zheng Zhang, Stephen Lin, and Baining Guo. Swin Transformer: Hierarchical vision transformer using shifted windows. In *ICCV*, 2021.

Jiasen Lu, Dhruv Batra, Devi Parikh, and Stefan Lee. ViLBERT: Pretraining task-agnostic visiolinguistic representations for vision-and-language tasks. In *NeurIPS*, 2019.

Jonathon Luiten, Aljosa Osep, Patrick Dendorfer, Philip Torr, Andreas Geiger, Laura Leal-Taixé, and Bastian Leibe. HOTA: A higher order metric for evaluating multi-object tracking. In *IJCV*, 2021.

Muhammad Maaz, Hanooona Rasheed, Salman Khan, and Fahad Shahbaz Khan. Video-ChatGPT: Towards detailed video understanding via large vision and language models. In *ACL*, 2024.

Anton Milan, Laura Leal-Taixé, Ian Reid, Stefan Roth, and Konrad Schindler. MOT16: A benchmark for multi-object tracking. *arXiv preprint arXiv:1603.00831*, 2016.

Eyal Molad, Eliahu Horwitz, Dani Valevski, Alex Rav Acha, Yossi Matias, Yael Pritch, Yaniv Leviathan, and Yedid Hoshen. Dreamix: Video diffusion models are general video editors. *arXiv preprint arXiv:2302.01329*, 2023.

Mathew Monfort, SouYoung Jin, Alexander Liu, David Harwath, Rogerio Feris, James Glass, and Aude Oliva. Spoken moments: Learning joint audio-visual representations from video descriptions. In *CVPR*, 2021.

Bryan A Plummer, Liwei Wang, Chris M Cervantes, Juan C Caicedo, Julia Hockenmaier, and Svetlana Lazebnik. Flickr30k entities: Collecting region-to-phrase correspondences for richer image-to-sentence models. In *ICCV*, 2015.

Alec Radford, Jong Wook Kim, Chris Hallacy, Aditya Ramesh, Gabriel Goh, Sandhini Agarwal, Girish Sastry, Amanda Askell, Pamela Mishkin, Jack Clark, et al. Learning transferable visual models from natural language supervision. In *ICML*, 2021.

Hanooona Rasheed, Muhammad Maaz, Sahal Shaji, Abdelrahman Shaker, Salman Khan, Hisham Cholakkal, Rao M Anwer, Eric Xing, Ming-Hsuan Yang, and Fahad S Khan. GLaMM: Pixel grounding large multimodal model. In *CVPR*, 2024.

Joseph Redmon, Santosh Divvala, Ross Girshick, and Ali Farhadi. You Only Look Once: Unified, real-time object detection. In *CVPR*, 2016.

Shaoqing Ren, Kaiming He, Ross Girshick, and Jian Sun. Faster R-CNN: Towards real-time object detection with region proposal networks. In *NeurIPS*, 2015.

---

Anna Rohrbach, Marcus Rohrbach, Ronghang Hu, Trevor Darrell, and Bernt Schiele. Grounding of textual phrases in images by reconstruction. In *ECCV*, 2016.

Mohit Shridhar, Jesse Thomason, Daniel Gordon, Yonatan Bisk, Winson Han, Roozbeh Mottaghi, Luke Zettlemoyer, and Dieter Fox. ALFRED: A benchmark for interpreting grounded instructions for everyday tasks. In *CVPR*, 2020.

Chen Sun, Austin Myers, Carl Vondrick, Kevin Murphy, and Cordelia Schmid. VideoBERT: A joint model for video and language representation learning. In *ICCV*, 2019.

Gemini Team, Rohan Anil, Sebastian Borgeaud, Jean-Baptiste Alayrac, Jiahui Yu, Radu Soricut, Johan Schalkwyk, Andrew M Dai, Anja Hauth, Katie Millican, et al. Gemini: a family of highly capable multimodal models. *arXiv preprint arXiv:2312.11805*, 2023.

Gemini Team, Petko Georgiev, Ving Ian Lei, Ryan Burnell, Libin Bai, Anmol Gulati, Garrett Tanzer, Damien Vincent, Zhufeng Pan, Shibo Wang, et al. Gemini 1.5: Unlocking multimodal understanding across millions of tokens of context. *arXiv preprint arXiv:2403.05530*, 2024.

Oriol Vinyals, Alexander Toshev, Samy Bengio, and Dumitru Erhan. Show and Tell: A neural image caption generator. In *CVPR*, 2015.

Haochen Wang, Cilin Yan, Shuai Wang, Xiaolong Jiang, Xu Tang, Yao Hu, Weidi Xie, and Efstratios Gavves. Towards Open-Vocabulary Video Instance Segmentation. In *ICCV*, 2023.

Jianfeng Wang, Zhengyuan Yang, Xiaowei Hu, Linjie Li, Kevin Lin, Zhe Gan, Zicheng Liu, Ce Liu, and Lijuan Wang. GIT: A generative image-to-text transformer for vision and language. In *TMLR*, 2022.

Junchi Wang and Lei Ke. LLM-Seg: Bridging image segmentation and large language model reasoning. In *CVPR*, 2024.

Nicolai Wojke, Alex Bewley, and Dietrich Paulus. Simple online and realtime tracking with a deep association metric. In *IEEE International Conference on Image Processing*, 2017.

Jialian Wu, Jianfeng Wang, Zhengyuan Yang, Zhe Gan, Zicheng Liu, Junsong Yuan, and Lijuan Wang. Grit: A generative region-to-text transformer for object understanding. In *ECCV*, 2024.

Junbin Xiao, Angela Yao, Yicong Li, and Tat-Seng Chua. Can I trust your answer? Visually grounded video question answering. In *CVPR*, 2024.

Antoine Yang, Antoine Miech, Josef Sivic, Ivan Laptev, and Cordelia Schmid. Just Ask: Learning to answer questions from millions of narrated videos. In *ICCV*, 2021.

Antoine Yang, Antoine Miech, Josef Sivic, Ivan Laptev, and Cordelia Schmid. TubeDETR: Spatio-temporal video grounding with transformers. In *CVPR*, 2022a.

Zhao Yang, Jiaqi Wang, Yansong Tang, Kai Chen, Hengshuang Zhao, and Philip HS Torr. LAVT: Language-aware vision transformer for referring image segmentation. In *CVPR*, 2022b.

Licheng Yu, Zhe Lin, Xiaohui Shen, Jimei Yang, Xin Lu, Mohit Bansal, and Tamara L Berg. MAttNet: Modular attention network for referring expression comprehension. In *CVPR*, 2018.

Zhou Yu, Jun Yu, Yuhao Cui, Dacheng Tao, and Qi Tian. Deep modular co-attention networks for visual question answering. In *CVPR*, 2019.

Haobo Yuan, Xiangtai Li, Tao Zhang, Zilong Huang, Shilin Xu, Shunping Ji, Yunhai Tong, Lu Qi, Jiashi Feng, and Ming-Hsuan Yang. Sa2VA: Marrying SAM2 with LLaVA for dense grounded understanding of images and videos. *arXiv preprint*, 2025.

Rowan Zellers, Ximing Lu, Jack Hessel, Youngjae Yu, Jae Sung Park, Jize Cao, Ali Farhadi, and Yejin Choi. MERLOT: Multimodal neural script knowledge models. In *NeurIPS*, 2021.

Hao Zhang, Hongyang Li, Feng Li, Tianhe Ren, Xueyan Zou, Shilong Liu, Shijia Huang, Jianfeng Gao, Leizhang, Chunyuan Li, et al. LLaVa-Grounding: Grounded visual chat with large multimodal models. In *ECCV*, 2024.

---

Susan Zhang, Stephen Roller, Naman Goyal, Mikel Artetxe, Moya Chen, Shuohui Chen, Christopher Dewan, Mona Diab, Xian Li, Xi Victoria Lin, et al. OPT: Open Pre-trained Transformer language models. *arXiv preprint arXiv:2205.01068*, 2022a.

Yifu Zhang, Peize Sun, Yi Jiang, Dongdong Yu, Fucheng Weng, Zehuan Yuan, Ping Luo, Wenyu Liu, and Xinggang Wang. ByteTrack: Multi-Object Tracking by Associating Every Detection Box. In *ECCV*, 2022b.

Zhu Zhang, Zhou Zhao, Yang Zhao, Qi Wang, Huasheng Liu, and Lianli Gao. Where does it exist: Spatio-temporal video grounding for multi-form sentences. In *CVPR*, 2020.

Xingyi Zhou, Dequan Wang, and Philipp Krähenbühl. Objects as points. *arXiv preprint arXiv:1904.07850*, 2019.

Xingyi Zhou, Tianwei Yin, Vladlen Koltun, and Philipp Krähenbühl. Global tracking transformers. In *CVPR*, 2022.

Xingyi Zhou, Anurag Arnab, Chen Sun, and Cordelia Schmid. Dense video object captioning from disjoint supervision. In *ICLR*, 2025.

Wenqi Zhu, Jiale Cao, Jin Xie, Shuangming Yang, and Yanwei Pang. CLIP-VIS: Adapting CLIP for Open-Vocabulary Video Instance Segmentation. *IEEE Transactions on Circuits and Systems for Video Technology*, 2024.

Yuke Zhu, Oliver Groth, Michael Bernstein, and Li Fei-Fei. Visual7W: Grounded question answering in images. In *CVPR*, 2016.

## A APPENDIX

In this appendix, we show qualitative results from our method in Section A.1, present additional ablations in Section A.2, discuss failure cases and limitations in Section A.3, and share more details about the datasets, the method, and the implementation in Section A.4.

### A.1 QUALITATIVE RESULTS

We show qualitative DVOC results from MaskCaptioner on the LV-VIS (Wang et al., 2023) dataset with (mask, caption) pairs predictions, and on the VidSTG dataset (Zhang et al., 2020) with (box, caption) pairs in Figures 5 and 6 respectively. These examples show that MaskCaptioner has learned to predict captions that focus on the localized objects while integrating high-level scene understanding.

On LV-VIS (Fig. 5), MaskCaptioner is able to produce descriptive captions for each objects including related context, even in the case of a scene including a high number of objects. We note that, when tuned on VidSTG (see Fig. 6), MaskCaptioner produces less informative and less descriptive captions. This is due to the VidSTG annotation captions being designed for grounding rather than for captioning or DVOC, and thus being only little descriptive or informative, and overlooking to the global context. In contrast, when trained on LVISCap and LV-VISCap, MaskCaptioner visually generates much richer and accurate descriptions, further highlighting the value of our synthetic captions. Overall, MaskCaptioner effectively learns to jointly segment, detect, track and caption object trajectories.

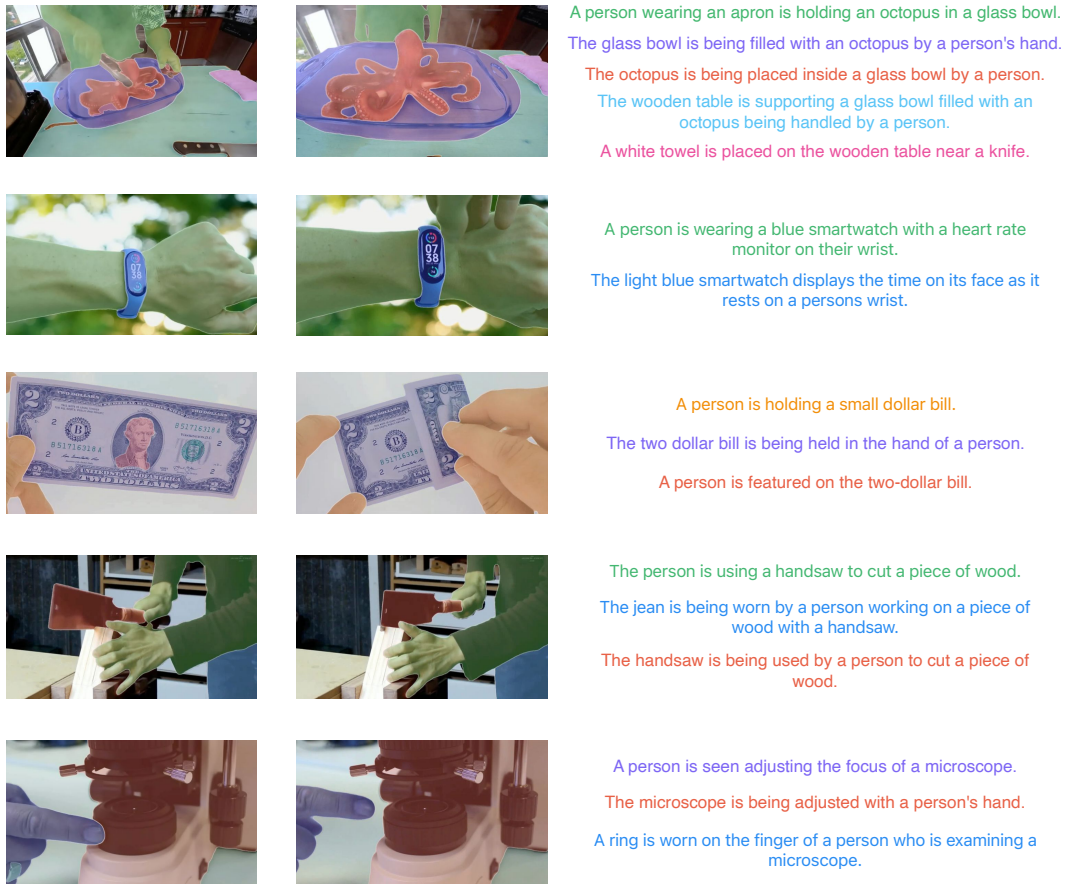


Figure 5: Qualitative examples, obtained with MaskCaptioner on the LV-VIS dataset.

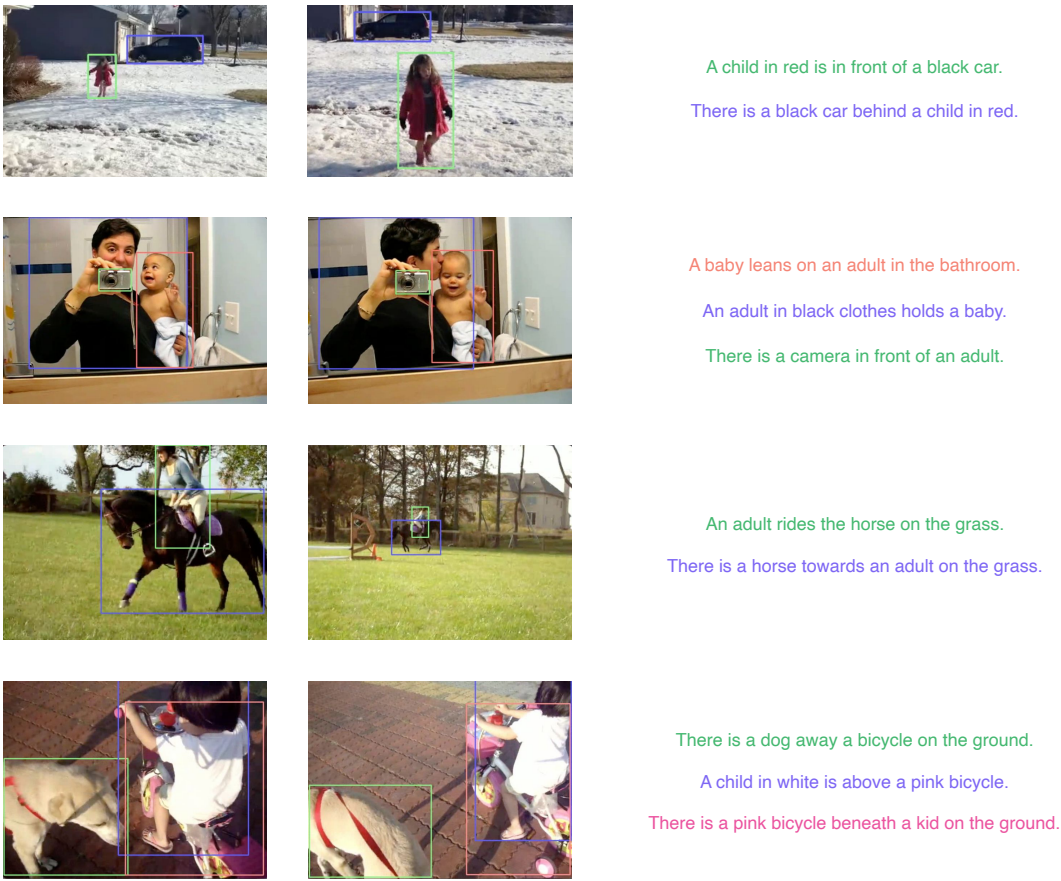


Figure 6: Qualitative examples, obtained with MaskCaptioner on the VidSTG dataset.

Table 9: **Impact of the prompting strategy on caption quality.** Scores are given by a human evaluator from 0 to 2 (incorrect, partially correct, or correct) on a subset from the LV-VIS validation set, and brought to 0-100 range. For the mask visual prompt experiments, we use our best prompt with either the object’s bounding boxes or center point coordinates as a localization cue in the text prompt.

| Visual prompt   | Prompting method           | Average rating | Rating percentage |      |       |
|-----------------|----------------------------|----------------|-------------------|------|-------|
|                 |                            |                | 0                 | 1    | 2     |
| bounding boxes  | single frame               | 26.8           | 66.3              | 13.9 | 19.9  |
|                 | + multiple frames          | 27.1           | 68.7              | 8.4  | 22.9  |
|                 | + detailed instructions    | 29.5           | 65.0              | 10.8 | 24.10 |
|                 | + category labels          | 80.7           | 10.8              | 16.9 | 72.3  |
|                 | + bounding box coordinates | 83.1           | 9.6               | 14.5 | 75.9  |
|                 | + bounding box area        | 84.3           | 7.8               | 15.7 | 76.5  |
|                 | + few shot examples        | <b>85.1</b>    | 9.1               | 11.5 | 79.4  |
| mask boundaries | center point coordinates   | 75.9           | 17.5              | 13.2 | 69.3  |
|                 | bounding box coordinates   | 77.1           | 15.7              | 14.5 | 69.9  |

## A.2 ADDITIONAL ABLATIONS

**Prompting strategy.** In Table 9, we show the distribution of ratings given by the human annotator depending on the prompting strategy. Using the box visual prompt yields a better focus on the queried object and more correct object captions. Importantly, giving the category labels in the prompt helps the model to generate more accurate object captions. Overall, the rate of correct captions with the best prompt indicates good quality for our synthetic object captions.

**Tracking module.** In Table 10, we show that the top-k enhanced tracking (Zhu et al., 2024) is important for tracking objects effectively on the challenging VidSTG dataset (Zhang et al., 2020), as seen in the AssA, CapA and CHOTA scores. We attribute this difference to the numerous objects that disappear for a significant number of frames in the long videos of VidSTG. The top-K approach uses a memory bank of tracked queries that helps keeping track of these entities, while they are lost using the  $i$  to  $i + 1$  tracking from OVFormer (Fang et al., 2025).

Table 10: **Impact of the tracking module on VidSTG DVOC.**

| Tracking method                          | CapA        | DetA        | AssA        | CHOTA       |
|--|-------------|-------------|-------------|-------------|
| OVFormer module (Fang et al., 2025)      | 51.9        | <b>67.0</b> | 58.2        | 58.7        |
| Top-K enhanced module (Zhu et al., 2024) | <b>52.7</b> | 66.8        | <b>71.0</b> | <b>63.0</b> |

## A.3 FAILURE CASES AND LIMITATIONS

### A.3.1 FAILURE CASES



Figure 7: Some DVOC failure cases of MaskCaptioner observed on the LV-VIS dataset.

We observe 3 main types of failure cases for our approach and illustrate them in Figure 7:

**(i) Recognition error:** in the case of ambiguous context, blurred instance or rare categories, MaskCaptioner might fail to recognize the object it is describing, sometimes leading to a wrong denomination

---

(e.g. here, a rare "pair of tongs" is incorrectly denominated as "knife"). **(ii) Inconsistent captions** : in similar situations, the captions produced by MaskCaptioner can be inconsistent when referring to the same object in different captions. **(iii) Detection/segmentation error** : In case of complex movement, appearance change or occlusion, MaskCaptioner sometimes fails to detect, segment, or track objects, leading to missing captions (e.g. here, the fish is not detected in the beak of the heron, and thus has no associated caption).

### A.3.2 LIMITATIONS

**Limitations.** While our approach outperforms the state-of-the-art in dense video object captioning, there is still room for improving localization and captioning. Localization sometimes fails, in particular for small objects. Furthermore, the automatically generated captions are, in some cases, too generic, and can mix up two objects of the same class in the video. Future work could investigate different automatic captioning techniques for DVOC, for example based on an approach such as Ref-SAV(Yuan et al., 2025), which generates captions in multiple steps to separate appearance from motion description. Eventually, objects in the videos often perform a single or few actions, and we believe that it is important for future works to build benchmarks with more complex object interactions, for instance with multiple action segments.

## A.4 ADDITIONAL DETAILS

### A.4.1 PROMPTING STRATEGY DETAILS

The full prompt template used to generate our LVISCap and LV-VISCap datasets is illustrated in Figure 8. For a video  $x$  with  $N$  objects, we prompt the VLM  $N$  times, and for each object  $j$  the prompt is composed in three parts: (i) the static system prompt  $p_s$  gives general instructions for object-level caption generation, practical rules, prompting format and an example, (ii) the user prompt  $p_u(j)$  depends on the example and contains textual annotation information to help the model describe objects and interactions accurately. These information notably contain target object positions, areas, category, and the categories of other objects in the scene, (iii) the visual prompt  $\hat{x}_j$  consists of 4 sampled frames with drawn bounding boxes for object  $j$ .

### A.4.2 DATASET DETAILS

**LVIS** (Gupta et al., 2019) is a large-vocabulary image instance segmentation dataset with a long-tail distribution of 1203 annotated categories, for a total of over 2.2 million annotations in 164k natural images. The dataset is split in a training set with 100k images and 1.2M annotations, a validation set with 19k images and 244k annotations, and two test sets with 19k images each.

**LV-VIS** (Wang et al., 2023) is a recent large-vocabulary video instance segmentation (VIS) benchmark. It comprises 4,828 videos with over 26k video segmentation masks from 1,196 object categories, with an average of over 5.4 objects per video. The data is split into a training set of 3,076 videos and 16k video-level annotations, a validation set of 837 videos and 3.7k annotations, and a test set with 908 videos.

**LVISCap** and **LV-VISCap** denote our extensions of LVIS and LV-VIS (see Section 3.1). LVISCap extends LVIS with a total of 1,488,354 synthetic captions, including 1,244,271 training annotations and 244,083 validation annotations. LV-VISCap includes a total of 19,717 synthetic captions for 16,017 training and 3,700 validation annotations. Note that in the absence of annotations on the test sets of LVIS and LV-VIS, we only extend the training and validation sets with captions, and use the validation set for evaluation.

**VidSTG**(Zhang et al., 2020) is a spatio-temporal video grounding dataset, containing 6,924 videos with 44,808 exhaustive trajectories annotations over 80 categories, as well as object sentence descriptions (for some objects and some timestamps only), which serve as queries for grounding. Zhou et al. (2025) repurposed the dataset for DVOC by using queries as captions, and by excluding annotations without captions during evaluation. Following Zhou et al. (2025), we sample 200 frames uniformly across each video for both training and evaluation. Overall, the repurposed VidSTG training set counts 28,275 object trajectories, with 15,182 object captions. The validation set, used for DVOC evaluation, includes 602 videos with 1,644 captions.

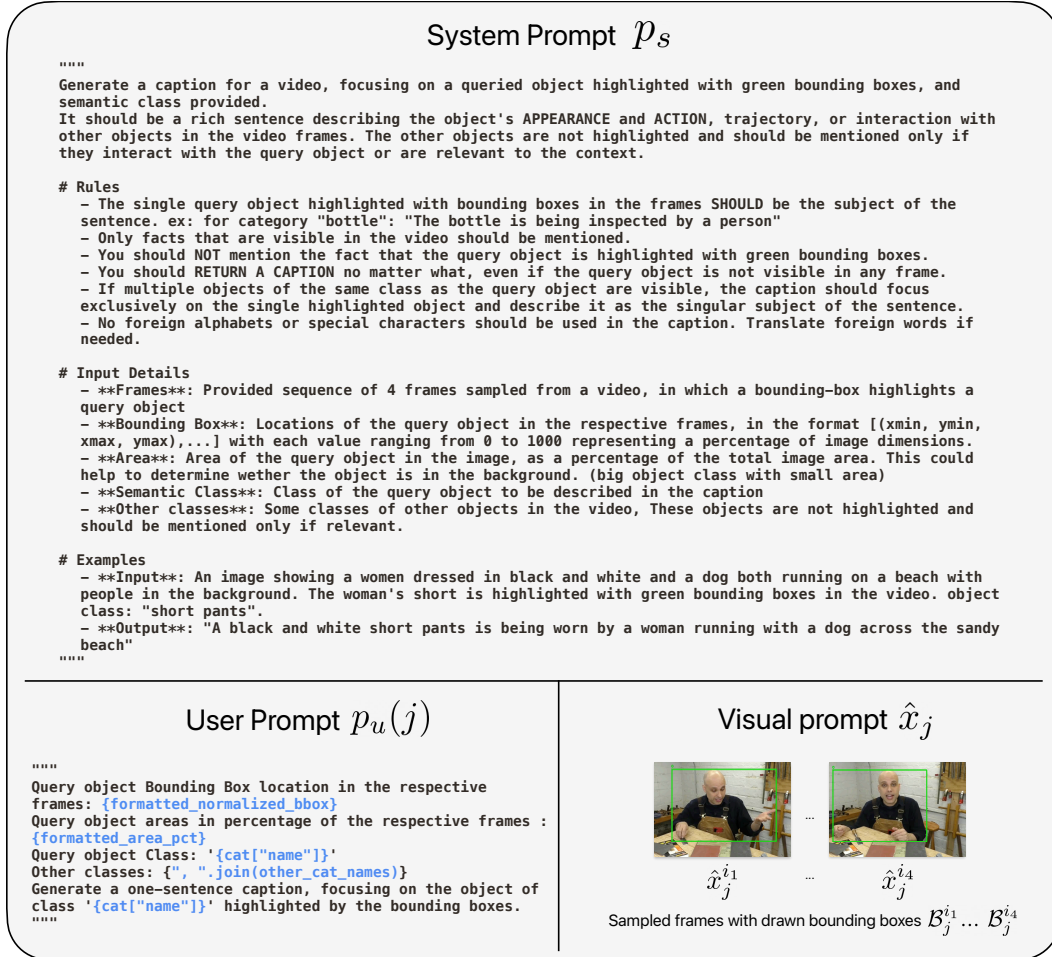


Figure 8: Prompt template used to generate synthetic object captions from video segmentation annotations for the LV-VIS dataset Wang et al. (2023). The system prompt  $p_s$  contains general instructions, while user prompt and visual prompt  $p_u(j)$  and  $\hat{x}_j$  are formatted with information from each annotation.

**Video Localized Narratives (VLN)** extends existing datasets with "narrations of actors actions" in videos. We use the subset from the UVO dataset, which contains 3 sparsely annotated frames with non exhaustive captions for a total of 5,136 training and 2,451 validation videos.

**BenSMOT** contains manually collected annotations of bounding box trajectories and associated captions, focusing exclusively on humans in videos. It includes an average of 2.2 instances per video, and counts 2,284 videos for training and 1,008 for evaluation.

#### A.4.3 MORE IMPLEMENTATION DETAILS

The visual backbone is initialized with weights pretrained on ImageNet-21K Deng et al. (2009) following OVFormer Fang et al. (2025), and the Mask2Former Cheng et al. (2022) weights are trained from scratch. The OVFormer classifier uses a frozen CLIP ViT-B/32 Radford et al. (2021) encoder. The captioning head is initialized with weights from BLIP-2 Li et al. (2023a) with frozen LLM OPT-2.7B Zhang et al. (2022a) following Chouduri et al. Choudhuri et al. (2024).

For all experiments except LV-VIS tuning, we first train the segmentation/detection model, then freeze it and tune the captioning head. Respectively for LVIS/VidSTG/LV-VIS we train for 440k/40k/22k for the first stage and 5k/2k/2k for the second stage. When tuning pretrained models on VidSTG/VLN/BenSMOT, we train the two stages for (15k, 2k)/(15k, 500)/(15k, 2k) steps, whereas for

---

LV-VIS, we end-to-end tune the model for  $2k$  steps. Experiments are run with a batch size of 8, except when using LVIS+COCO and LV-VIS where we use a batch size of 4 and for video-level tuning of the captioning head where we use a batch-size of 1. Experiments on LV-VIS are end-to-end trainings with clip-level supervision only. For VidSTG/VLN/BenSMOT experiments we use video-level tuning for captioning with temporal aggregation, with  $T_{\text{agg}} = 32/8/8$  respectively. For all experiments we train the model with  $k$  clips of size  $T = 2$ , and at inference use  $T = 5/1/1/1$ ,  $T_{\text{match}} = 1/100/20/40$ ,  $K_{\text{match}} = 1/7/5/7$  for LV-VIS/VidSTG/VLN/BenSMOT experiments respectively. For the largest dataset (COCO + LVIS) the optimization takes 2 days on 4 H100 GPUs.

Following OVFormer Fang et al. (2025), for all datasets we use an AdamW optimizer and the step learning rate schedule, with an initial learning rate of 0.0001 and a weight decay of 0.05, and apply a 0.1 learning rate multiplier to the backbone. We decay the learning rate at 0.9 and 0.95 fractions of the total number of training steps by a factor of 10. For respectively image/video datasets, we resize the shortest edge of the image to 800/480 for SwinB and 800/360 for ResNet for training and inference.